TENSION ALLOCATION IN THREE DIMENSIONAL WOUND ROLL

by

P. Hoffecker and J. K. Good
Oklahoma State University
USA

ABSTRACT

Much consideration has been given to the relationship between web line tension and the stresses they induce in three dimensional wound rolls. Three dimensional wound rolls are distinctive because their radial and circumferential stresses are not uniform across their width. The non-uniformity results from numerous factors including Cross Machine Direction variations in the core stiffness, web thickness, or web line tension. Whatever the source, ultimately they produce variations in the radius across the width. In order to maintain material continuity, the incoming layer must therefore conform to a winding roll that is non-uniform in radius across its width. This is accomplished when the applied web line tension allocates across the width in proportion to the roll's local radius, as it converts into the outside layer's circumferential stress. The tension concentrates in high regions and disperses in the low regions. The model presented herein combines axisymmetric finite element analysis with a radius based tension allocation algorithm in order to simulate the actual stresses in a three dimensional roll. The circumferential stresses across the width are iteratively made to sum to the web line tension boundary condition. Comparison with experimental data from three dimensional rolls shows the model captures the essence of the roll behavior. It thus confirms the existence of the radius dependent tension allocation.

NOMENCLATURE

$\overline{\mathbf{B}}$	FEM Transformation Vector
CMD	Cross Machine Direction
$\overline{\mathbf{D}}$	FEM Stress to Strain Matrix
E	Modulus of Elasticity
ESM	Element Stiffness Matrix
$\overline{\mathbf{F}}$	FEM Global Force Vector
$\overline{\mathbf{f}}$	Body Force Vector

FEM	Finite Element Model
G	Shear Modulus
$\overline{\mathbf{J}}$	Jacobian Matrix
$\overline{\mathbf{K}}$	FEM Global Stiffness Matrix
$\overline{\mathbf{L}}$	Concentrated Point Load Vector
P	Roll Pressure
$\overline{\mathbf{Q}}$, $\overline{\mathbf{q}}$	FEM Deformation Vector, Global and Elemental
R, r	Roll Radial Direction
$\overline{\mathbf{T}}$	Traction Vector
T_W	web tension, load/width
V_0	Incoming Web Velocity
Z, z	Roll CMD Direction
$\beta_1, \beta_2, \beta_0$	Multi-point Constraint Constants
$\overline{\epsilon}$	Strain Vector
θ	Roll Circumferential Direction, Roll Rotational Angle
$\overline{\sigma}$	Stress Vector
ω	Roll Rotational Rate
j	CMD Sector Index

INTRODUCTION

In industries that deal with wound rolls (generally known as web handlers), roll quality is of paramount importance. Web and wound roll defects are estimated to account for millions of dollars worth of product losses annually. As a result, wound roll quality prediction has been a major concern in the industry for many years. It is the reason that a number of web handling companies formed a consortium and started the Web Handling Research Center (WHRC) at Oklahoma State University. Wound roll quality prediction and improvement is the underlying theme of many publications. The early publications were all two dimensional; they only investigated the radial and circumferential stresses in wound rolls. Some of the more prominent ones include Pfeiffer's [1] in 1966, and Altmann [2] in 1968, which itself cites the importance of quality prediction and even mentions government sponsored funding conducted by Gutterman [3] dating back to 1959. More recent publications like Hakiel [4] in 1987, and Good and Pfeiffer [5] in 1992, also work to improve and predict two dimensional wound roll quality.

The three dimensional publications go one step further than the two dimensional ones by investigating if CMD variations affect the stresses throughout a wound roll. Collectively, their focus includes the compounding effects of web thickness variations which persist in the length direction, non-uniformities in the core's radius, changes in the core's stiffness, and CMD variations in web line tension. Kedl [6] addresses the web thickness and core radius variations by maintaining the outer layer's material compatibility when distributing the web line tension across the roll's width. The investigations of Hakiel in [7], and Cole and Hakiel in [8] accommodate CMD web thickness and core radius variations by ensuring each layer's allocated tensions sum to match the web line tension. Unfortunately, all three investigations suffer from a lack of continuity across the width. The more recent investigations by Lee and Wickert [9 and

10] focus on the impact of core stiffness variations under uniformly and non-uniformly applied web line tension respectively. None of these three dimensional investigations address CMD variations in the web's in-roll tension distribution, or its properties (other than radial modulus).

All of the three dimensional investigations determined that CMD variations cause concentrations in the roll's stresses. Because excessive stress concentrations can damage the web, it is certain the web handling industry would benefit greatly if they were able to accurately estimate the quality of a roll before it was even wound. The model presented here works to predict the stresses in wound rolls subject to CMD variations. By using quadrilateral finite elements with an inherent thickness, it addresses buildups that occur in discreet CMD locations (sectors). Tying the quadrilaterals together across the width provides continuity, and incorporates the interplay between sectors. The model accretes each layer onto the roll and iteratively adjusts the tension to match the winding tension. At the same time, coordinates, stresses, and radial moduli are updated to reflect the wound roll's state.

MODEL DERIVATION

An axisymmetric FEM addresses the necessary cross width continuity, stress concentrations, and thicknesses. In general, a finite element is a mathematical representation of a physical, geometric object. Axisymmetric finite elements represent materials in the two dimensional RZ plane, and then spin them around the Z axis in the θ direction to form a three dimensional shell

In this model, the axisymmetric elements are quadrilaterals. The deformations and strains, the corresponding stresses, and the material properties, can all vary in the R and Z directions, but can not vary in the θ direction. The invariance in the θ direction makes the representation symmetric about the Z axis, and is the source for the name axisymmetric. Physical variations in a wound roll are handled by placing multiple elements across the variation and thus subdividing it into smaller, well behaved portions. This provides the continuity across the roll.

The quadrilateral elements are conducive to representing a web's cross section. The element's four corners bracket the web layer's thickness, thereby following its profile across the width. Behaviors such as strain and stress are allowed to change linearly between the corners. At the same time, properties like moduli and Poisson's ratios remain uniform in an element. This trait makes adjacent elements handle the necessary variations in the cross machine and radial directions and provides for a different material stiffness in each element.

The elemental thicknesses are input into the model as values corresponding to a pre-specified number of equal cross width segments. To look like a web cross section they are transformed into a profile called the bi-linearly varying thickness profile shown in Figure 1.

FEMs derive from a minimum potential energy formulation [11]. The potential energy in a conservative system is the summation of its strain energy and its work potential. At its minimum, the potential energy formulation represents a unique, stable configuration. Taking the derivative of the formulation with respect to the deformations, and setting the result to zero, yields this minimum configuration. The deformations that satisfy the minimum configuration give the deformed state of the system.

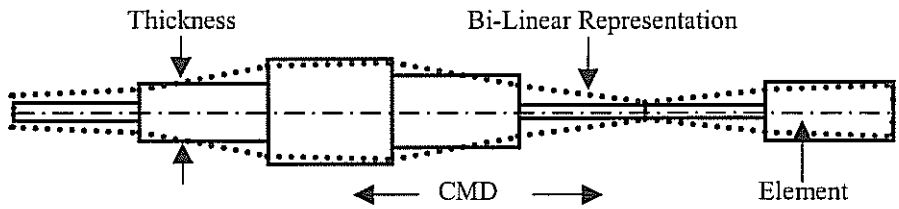

Figure 1 – Web's CMD Bi-Linear Thickness Representation

The strain energy contribution to the potential energy comes from a material's inherent behavior. Linear elastic materials develop a strain energy per unit volume equal to $1/2\,\bar{\sigma}^T\bar{\epsilon}$. Thus, the total strain energy results from integrating over the volume, as depicted in equation {1}.

$$U = \frac{1}{2}\int_V \bar{\sigma}^T\bar{\epsilon}\,dV \qquad \{1\}$$

To simplify this expression, we utilize the fact that each material (and necessarily each element representing that material) abides by constitutive equations relating its stress and strain. The fully three dimensional, orthotropic, polar constitutive equations are given in equation {2}.

$$\begin{bmatrix} \varepsilon_{rr} \\ \varepsilon_{\theta\theta} \\ \varepsilon_{zz} \\ \varepsilon_{r\theta} \\ \varepsilon_{rz} \\ \varepsilon_{\theta z} \end{bmatrix} = \begin{bmatrix} 1/E_r & -\nu_{\theta r}/E_\theta & -\nu_{zr}/E_z & 0 & 0 & 0 \\ -\nu_{r\theta}/E_r & 1/E_\theta & -\nu_{z\theta}/E_z & 0 & 0 & 0 \\ -\nu_{rz}/E_r & -\nu_{\theta z}/E_\theta & 1/E_z & 0 & 0 & 0 \\ 0 & 0 & 0 & 2/G_{r\theta} & 0 & 0 \\ 0 & 0 & 0 & 0 & 2/G_{rz} & 0 \\ 0 & 0 & 0 & 0 & 0 & 2/G_{\theta z} \end{bmatrix} \begin{bmatrix} \sigma_{rr} \\ \sigma_{\theta\theta} \\ \sigma_{zz} \\ \sigma_{r\theta} \\ \sigma_{rz} \\ \sigma_{\theta z} \end{bmatrix} \qquad \{2\}$$

Note, this expansion introduces the modulus of rigidity (or shear modulus), G, in three different coordinate orientations. The inverse of the matrix in equation {2}, relates the stress vector to the strains, and is denoted $\bar{\mathbf{D}}$.

All of the finite elements which are in the wound roll model, are systematically linked onto an undeformed, representative, quadrilateral element in a model space. This element is referred to as the master element. Just like the physical RZ plane, the model space is a two dimensional plane, but it uses a different set of orthogonal coordinates referred to as the natural coordinates, ξ and η. The master element is sized in the model space so that both natural coordinates range from -1 to 1. The deformations of the master element's four corners make up the deformation vector $\bar{\mathbf{q}}$. Values like strain require the use of the Jacobian matrix $\bar{\mathbf{J}}$, and its determinant to transform back and forth from the model space to the physical space. As seen in equation {3}, the Jacobian directly relates a change in the finite element's R and Z axes, to a change in the master element's ξ and η axes.

$$\overline{\mathbf{J}} = \begin{bmatrix} \frac{\delta R}{\delta \xi} & \frac{\delta Z}{\delta \xi} \\ \frac{\delta R}{\delta \eta} & \frac{\delta Z}{\delta \eta} \end{bmatrix} \qquad \{3\}$$

The quadrilateral's strain in the RZ plane can now be calculated. Note that because it is a planar element, it inherently has no out-of-plane strains. Its in-plane strains come from using the transformation matrix, $\overline{\mathbf{B}}$, in the succinct expression for strain shown in equation {4}.

$$\overline{\epsilon} = \overline{\mathbf{B}}\overline{\mathbf{q}} \qquad \{4\}$$

Substituting the strain (and its equivalent stress from equation {2}) directly into equation {1}, performing the transpose on the leading $\overline{\mathbf{D}}\overline{\mathbf{B}}\overline{\mathbf{q}}$ term, and moving the $\overline{\mathbf{q}}$ out of the integral produces equation {5}.

$$U = \frac{1}{2}\overline{\mathbf{q}}^T \int_V \overline{\mathbf{B}}^T \overline{\mathbf{D}}^T \overline{\mathbf{B}}\, dV\, \overline{\mathbf{q}} \qquad \{5\}$$

Further specializations develop this generic strain energy expression into an axisymmetric formulation. The integral over the volume splits into three, one dimensional integrals over the R, Θ, and Z directions. The R and Z integrals cover the area in the quadrilateral's plane. The Θ integral provides the axisymmetry through the full 0 to 2π revolution about the Z axis. The circumference of the revolution depends on the radius, r, of the quadrilateral, so the integral results in a 2πr factor. The revolution produces continuity around the circumference, and allows the planar quadrilateral to represent three dimensional shells. The axisymmetric formulation accounts for the circumferential stresses by appending the circumferential strain expression (shown below as equation {6}, with radial deformation u)

$$\varepsilon_{\theta\theta} = \frac{u}{r} \qquad \{6\}$$

onto equation {4}. Thus the "planar formulation" ends up with an out-of-plane strain. Then, to make the integrals consistent with the $\overline{\mathbf{B}}^T\overline{\mathbf{D}}^T\overline{\mathbf{B}}$ matrices, they are converted to natural coordinates via the substitution $dr\, dz = det\, \overline{\mathbf{J}}\; d\xi\, d\eta$.

In practice, the strain energy is captured through the use of an element stiffness matrix (ESM). The ESM is the eight by eight matrix which results from the term in brackets in equation {7}, which is the strain energy's updated expression.

$$U = \sum_e \frac{1}{2}\overline{\mathbf{q}}^T \left[2\pi \int_{-1}^{1} \int_{-1}^{1} \overline{\mathbf{B}}^T \overline{\mathbf{D}}\overline{\mathbf{B}} \det \overline{\mathbf{J}}\, r\, d\xi\, d\eta \right] \overline{\mathbf{q}} \qquad \{7\}$$

For practical implementation, the model uses two-point Gaussian Quadrature to approximate the two integrals. It would be unwieldy to find a closed form solution, since

the direct expansion of the bracketed term is quite complex. Assembling together all the element stiffness matrices produces a Global Stiffness Matrix (GSM), denoted $\overline{\mathbf{K}}$.

The work potential contribution to the potential energy arises from any of three general load categories applied to the system. Concentrated point loads ($\overline{\mathbf{L}}$) are forces that act on a single point. Body forces ($\overline{\mathbf{f}}$), like gravity, are loads distributed throughout a volume. Traction forces ($\overline{\mathbf{T}}$) are loads distributed over a surface area, and are the most significant and common loadings found in wound rolls. The work potential is given in equation {8}.

$$WP = -\sum \overline{\mathbf{q}}^T \left[2\pi \int_{-1}^{1} \int_{-1}^{1} \overline{\mathbf{f}}\, r \det \overline{\mathbf{J}}\, d\xi\, d\eta + 2\pi \int_{l} \overline{\mathbf{T}}\, r\, dl + \overline{\mathbf{L}} \right] \qquad \{8\}$$

If there is more than one load of a particular category, the equation must be expanded to include a formulation for each one. Therefore there can be multiple $\overline{\mathbf{L}}$ entries, for example. As a side note, all of the load categories above must be consistent with the locations they influence. In the same way the strain energy was contained in $\overline{\mathbf{K}}$, the work potential from the applied loads is contained by a global force vector $\overline{\mathbf{F}}$. And, just like for $\overline{\mathbf{K}}$, the global force vector merges the contributions of all the elements in the roll.

RADIUS BASED TENSION ALLOCATION

The primary load source in a centerwound roll, the web line tension, is not directly compatible with an axisymmetric formulation. It is indeed a traction force distributed over the web surface, but all the load categories in equation {8} must be in the plane of the element. The web line tension, however, is perpendicular to the element's RZ plane.

Multi-point constraints are needed to construct the final wound roll model. In the actual wound roll, each layer connects to layers above or below it through physical contact. But in the model, the layers are not inherently linked. Tying them together is accomplished by populating $\overline{\mathbf{K}}$ with a multi-point constraint equation like equation {9}.

$$\beta_1 Q_{P1} + \beta_2 Q_{P2} = \beta_0 \qquad \{9\}$$

Multi-point equations work by setting up a relationship between two previously independent points in the roll. The expression's Q terms refer to the degrees of freedom associated with the two points (1 and 2). The terms are numbered in the entire (global) wound roll, and are placed in the global deformation vector $\overline{\mathbf{Q}}$. The β terms are constants which ratio their corresponding degrees of freedom against each other. For example, if two layers' nodes are in contact, and are to move in concert, β_1 is set to -1, β_2 to 1, and β_0 to 0. This reduces equation {9} to $Q_{P2} = Q_{P1}$, and locks the two degrees of freedom together. The multi-point constraint equation is a modification of the potential energy formulation. It does not actually contribute to either the system's strain energy, or its work potential, but its components conveniently fit into their formulations. and are placed in $\overline{\mathbf{K}}$ or $\overline{\mathbf{F}}$.

The web line tension is enforced indirectly by using a multi-point constraint to interfere a new layer into the roll. The interference acts to compress the roll, while the roll reacts and expands the new layer. The sum total of the inward compression and the outward expansion equals the imposed interference, and leaves the new layer's inner

surface stretched over the roll's outer surface. The greater the layer's interference, the larger the resulting tension will be. To impose the interference, β_1 is -1, and β_2 is still 1, while β_0 is now equal to the interference. Just as they did for the multi-point constraint links between the layers, the β_1,and β_2 values populate $\overline{\mathbf{K}}$, while the β_0 terms insert into $\overline{\mathbf{F}}$. A physical depiction of the interference can be seen in Figure 2.

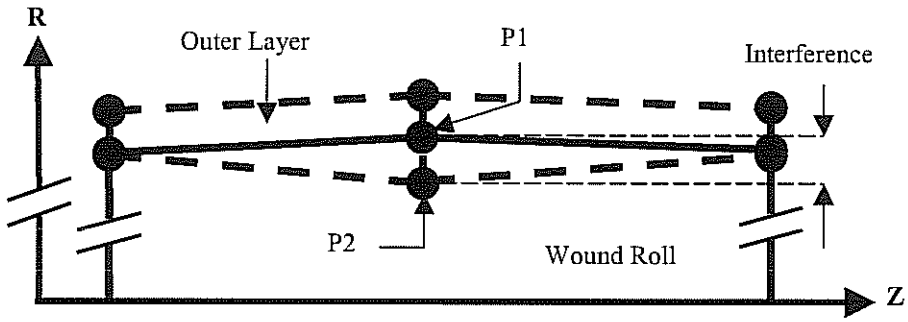

Figure 2 – Schematic Depiction of Layer Interference

The amount of tension partitioned out to the nodes is based on conserving circumferential material. Since each web layer remains continuous across the roll width, the amount of material passing onto the roll must be the same at all CMD locations. Otherwise, part of the web cross section would advance ahead of the rest, leaving the web's center dangling in the free-span while the edges were on the roll, for example! For an unstrained material, the amount that passes onto the roll, in one revolution, equals the circumference of the roll at that moment. For less than one revolution, the amount is the arc length r θ. Where r is the radius, and θ is the angle of rotation. The rotational angle encountered by all the locations across the width is, by definition, the same. Thus, for each location across the width to have the same r θ, means that all the radii would have to be the same too! And, such would be the case in the absence of strain. However, the strains across the width are not equal. They circumferentially stretch the web in proportion to the local tension. Web that is wound on a larger local radius will have a greater arc length, and a corresponding velocity lag behind its neighboring material. In an effort to maintain material compatibility with the surrounding web layer , this will cause the web to stretch locally. The local stretch is a local strain and a corresponding stress. Thus, each CMD location's radius provides the means to determine how much web line tension it should receive. This is the same method used by Kedl [6].

The model performs the allocation by scaling the location's circumferential velocity to the web's overall surface velocity as shown in equation {10}.

$$\varepsilon_{\theta\theta,j} = 1 - \frac{V_0\left(1-\varepsilon_{\theta\theta,0}\right)}{R_j\omega} \qquad \{10\}$$

Here $\varepsilon_{\theta\theta,j}$ represents the strain at widthwise location j in the outer layer of the roll, which has radius R_j. V_0 and $\varepsilon_{\theta\theta,0}$ are the web velocity, and machine direction strain, at a location far enough upstream that they can be considered uniform. denote individual 2D roll strains versus the incoming web strain respectively. The variable ω represents the rotational rate of the wound roll. As the roll accretes (winds), the radius at location j

changes, and so its portion of the web line tension is altered. Each layer's resulting tension and pressure compresses the layers below it, alters its stresses, and changes the radius of the roll.

Each location's radial position establishes its relative tension portion while the layer's total tension iterates to match web line tension. Using the arc length calculation, the tension and then the strain needed at each location across the width are first determined. Then from equation {6}, the new layer's initial interferences, in expression {9}, are estimated. Next, the model is solved. If the resulting sum of the tensions across the width does not equal the web line tension, all the interferences are equally scaled up or down. The roll and new layer are reset, and the scaled interference is imposed. This process repeats until the tension summation converges to the web line tension. The radial moduli are adjusted during the interference iteration as well. After finding each potential solution set, the radial moduli are recalculated throughout the wound roll. The flowchart in Figure 3 lays out the model's general progression.

SIMULATING WOUND ROLLS

Determining the stable energy configuration or "solving the model", calculates the deformations throughout the roll in its current configuration. With the roll's layers, core, and connections combined into $\overline{\mathbf{K}}$, the external loads and interferences taken care of by $\overline{\mathbf{F}}$, and the unknown deformations represented as $\overline{\mathbf{Q}}$, the roll's configuration becomes a finite element system, equation {11}.

$$\overline{\mathbf{F}} = \overline{\mathbf{KQ}} \qquad \{11\}$$

Every new layer accreted onto the roll incrementally reconfigures the entire roll. The deformations found by solving the system in {11} are a cascading reaction to the interference of only the outer layer. They are not the total deformations seen by the nodes when the entire roll is finished, but rather a snapshot of an intermediate state. In the comprehensive sense of the wound roll, they are better thought of as $\delta\overline{\mathbf{Q}}$.

The sum total of a node's $\delta\overline{\mathbf{Q}}$, from every time the system is solved, is that node's true total deformation. The model does not explicitly track the sum total delta deformations, but rather is concerned with hoe each $\delta\overline{\mathbf{Q}}$ converts to a $\delta\overline{\epsilon}$, and a corresponding $\delta\overline{\sigma}$. The $\delta\overline{\sigma}$ are summed instead, to produce the roll's comprehensive stress components σ_{rr}, σ_{zz}, σ_{rz}, and $\sigma_{\theta\theta}$. In that sense, the constitutive equations {2} for any one solution set of the accreting wound roll, are better represented as seen in equation {12}.

$$\begin{bmatrix} \delta\varepsilon_{rr} \\ \delta\varepsilon_{\theta\theta} \\ \delta\varepsilon_{zz} \\ \delta\varepsilon_{rz} \end{bmatrix} = \begin{bmatrix} 1/E_r & -\nu_{\theta r}/E_\theta & -\nu_{zr}/E_z & 0 \\ -\nu_{\theta r}/E_\theta & 1/E_\theta & -\nu_{z\theta}/E_z & 0 \\ -\nu_{zr}/E_z & -\nu_{z\theta}/E_z & 1/E_z & 0 \\ 0 & 0 & 0 & 2/G_{rz} \end{bmatrix} \begin{bmatrix} \delta\sigma_{rr} \\ \delta\sigma_{\theta\theta} \\ \delta\sigma_{zz} \\ \delta\sigma_{rz} \end{bmatrix} \qquad \{12\}$$

Summing the stresses instead of the deformations was not a random choice. The total σ_{rr} values are needed to determine an element's current E_r, which is state dependent on σ_{rr}.

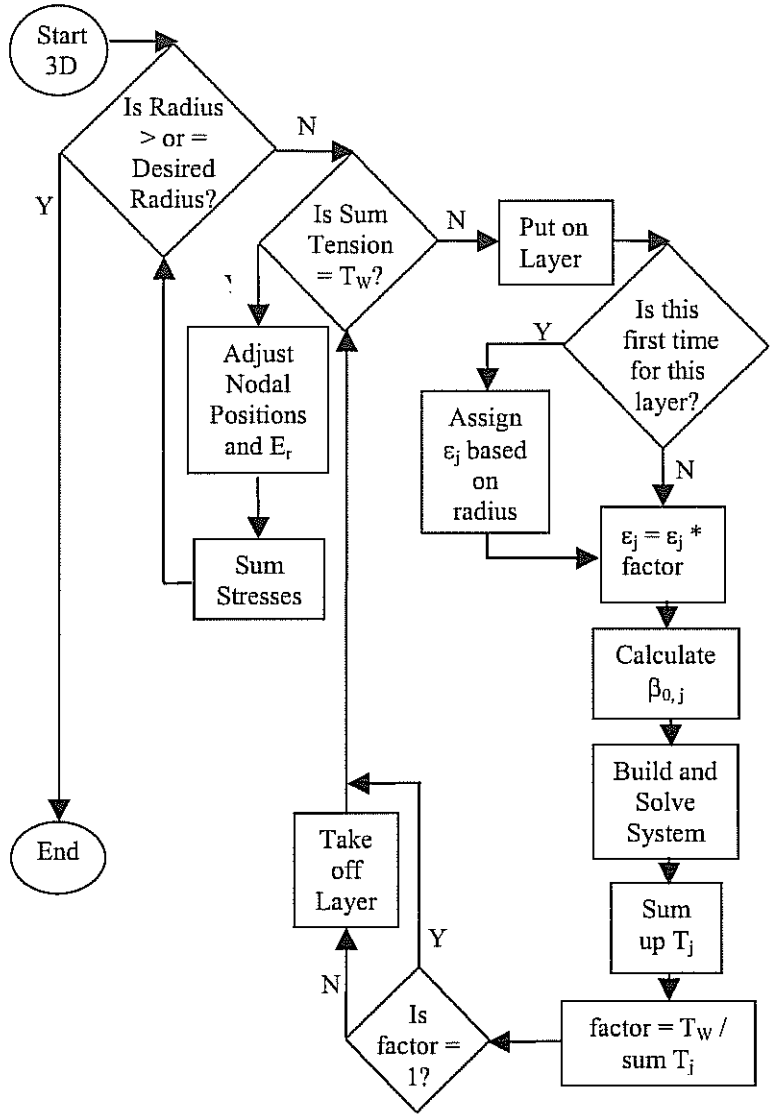

Figure 3 – Layer Accretion and Tension Iteration Flowchart

The model is designed to accommodate various wound roll configurations so it can be used as a design tool. The core is represented as a hollow, uniform thickness cylinder. The radial thickness can be adjusted to match the wall thickness of the roll's actual core. The model divides the thickness into two radially stacked layers to facilitate radial variations in its stresses. The core's width can be made larger than the web's width, as is common in winding.

This makes the model more realistic, and permits axial behavior, such as plane strain to plane stress transitions. It also provides a way to distance the web material away from the core supports. Many models simply represent the core as a composite stiffness value

or as an isotropic shell. The axisymmetric formulation will allow it to be orthotropic if desired.

There are a number of inputs necessary in addition to those previously mentioned for the core, and for the thickness profile. The desired roll radius is the radius the model uses as a target to stop the wind. Note that the model automatically accounts for the compression in the roll, during winding. Thus, a highly compressible material will wind on more layers to reach the same target radius as a less compressible material. Of course, the web's material properties, especially its radial modulus must be given. They are incorporated directly into the ESMs. The E_r representation used in the examples is from [8] and is given in equation {13}.

$$E_r = C_0\left(1 - e^{\frac{-P}{C_1}}\right) \qquad \{13\}$$

RESULTS

During the model development, results were compared to known sources for accuracy. The cylindrical core was developed first and checked against the Lekhnitskii classical expressions [12] that have been modified for consistent nomenclature and given in equations {14}, {15}, and {16}.

$$\sigma_{rr} = \left[\frac{P_{In}\left(\frac{R_{In}}{R_{Ex}}\right)^{\psi+1} - P_{Ex}}{1-\left(\frac{R_{In}}{R_{Ex}}\right)^{2\psi}}\right]\left(\frac{r}{R_{Ex}}\right)^{\psi-1} - \left[\frac{P_{In} - P_{Ex}\left(\frac{R_{In}}{R_{Ex}}\right)^{\psi-1}}{1-\left(\frac{R_{In}}{R_{Ex}}\right)^{2\psi}}\right]\left(\frac{R_{In}}{R_{Ex}}\right)^{\psi+1}\left(\frac{R_{Ex}}{r}\right)^{\psi+1} \qquad \{14\}$$

$$\sigma_{\theta\theta} = \left[\frac{P_{In}\left(\frac{R_{In}}{R_{Ex}}\right)^{\psi+1} - P_{Ex}}{1-\left(\frac{R_{In}}{R_{Ex}}\right)^{2\psi}}\right]\psi\left(\frac{r}{R_{Ex}}\right)^{\psi-1} + \left[\frac{P_{In} - P_{Ex}\left(\frac{R_{In}}{R_{Ex}}\right)^{\psi-1}}{1-\left(\frac{R_{In}}{R_{Ex}}\right)^{2\psi}}\right]\psi\left(\frac{R_{In}}{R_{Ex}}\right)^{\psi+1}\left(\frac{R_{Ex}}{r}\right)^{\psi+1} \qquad \{15\}$$

$$u = \frac{R_{Ex}}{1-\left(\frac{R_{In}}{R_{Ex}}\right)^{2\psi}}\left[\begin{array}{l}\left(P_{In}\left(\frac{R_{In}}{R_{Ex}}\right)^{\psi+1} - P_{Ex}\right)\left(\psi - \nu_{\theta r}\right)\left(\frac{r}{R_{Ex}}\right)^{\psi} + \\ \left(P_{In} - P_{Ex}\left(\frac{R_{In}}{R_{Ex}}\right)^{\psi-1}\right)\left(\psi + \nu_{\theta r}\right)\left(\frac{R_{In}}{R_{Ex}}\right)^{\psi+1}\left(\frac{R_{Ex}}{r}\right)^{\psi}\end{array}\right] \qquad \{16\}$$

$$with\ \psi = \sqrt{\frac{E_\theta}{E_r}}$$

The core's inside radius and pressure are given as R_{In} and P_{In}, while the external values are R_{Ex}, and P_{Ex}. The variable r is the radius (between R_{In} and R_{Ex}) at which the equations are being evaluated. The square root of the modulus ratio is represented by ψ

for simplification. All three equations apply specifically to orthotropic, thick walled cylinders like the wound roll core. As can be seen in Figure 4, the model's results matched the expressions closely.

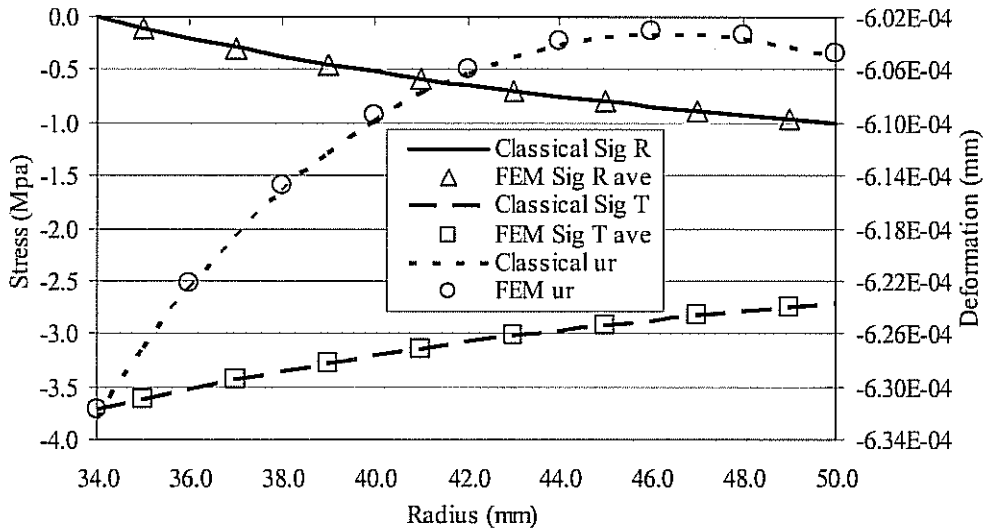

Figure 4 - Comparison of Classical and FEM Solutions of an Orthotropic, Annular Ring under External Pressure

The publication by Cole and Hakiel [8] provides experimental results to match against the axisymmetric model. They determine the thickness variation across the width for two, 25.4 cm wide webs, referred to as A and B. (Their webs are a 0.102 mm thick, PET material, with radial modulus coefficients C_0 = 2.4949 GPa, and C_1 = 8.6496 MPa.) Then they wind them on an aluminum, instrumented core at 3.5 N/cm and 7 N/cm winding tensions, up to 38.1 cm in diameter. During the wind they stop the roll a few times and measure the radius across the width. When the winding is done they measure the radial pressures on the instrumented core. Figure 5 below shows the CMD thickness profile they reported for their web A.

The radial pressure results from the axisymmetric model are plotted in Figure 6 against values they measured at the core, and the results of their own three dimensional model.

It is apparent that the axisymmetric model did well in predicting the radial pressure behavior across the entire width. The peak values do exceed the measured values around the eight cm CMD location, but this is due in part to the fact that the measured values apply to 2.54 cm wide segments. The axisymmetric model results are for 1.27 cm wide segments. When the two adjacent segments in each 2.54 cm width are averaged, the axisymmetric model's core pressures compare almost exactly to the measured values.

Since it is important to accurately predict a wound roll's outside radius across its width, the model also tracks the radii. Figure 7 plots the model's CMD radial profile.

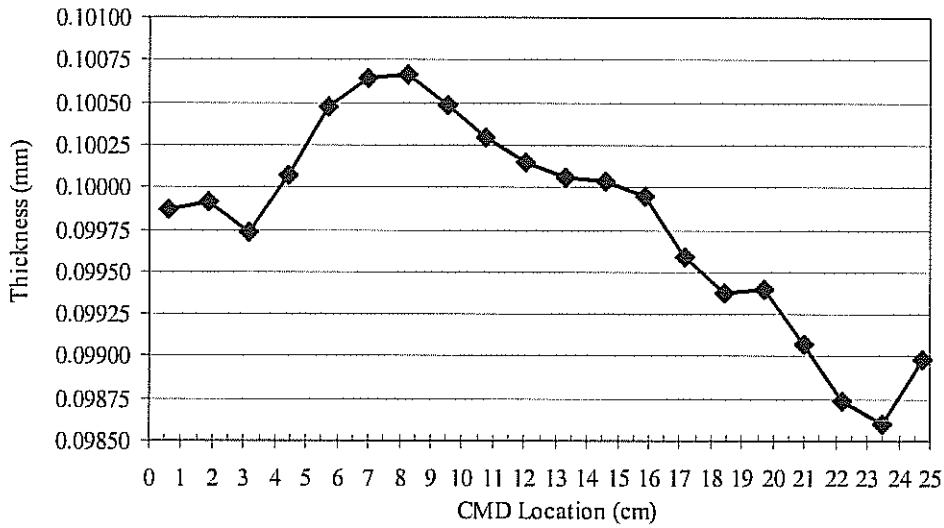

Figure 5 - CMD Thickness Profile for Cole & Hakiel [8], PET Web A.

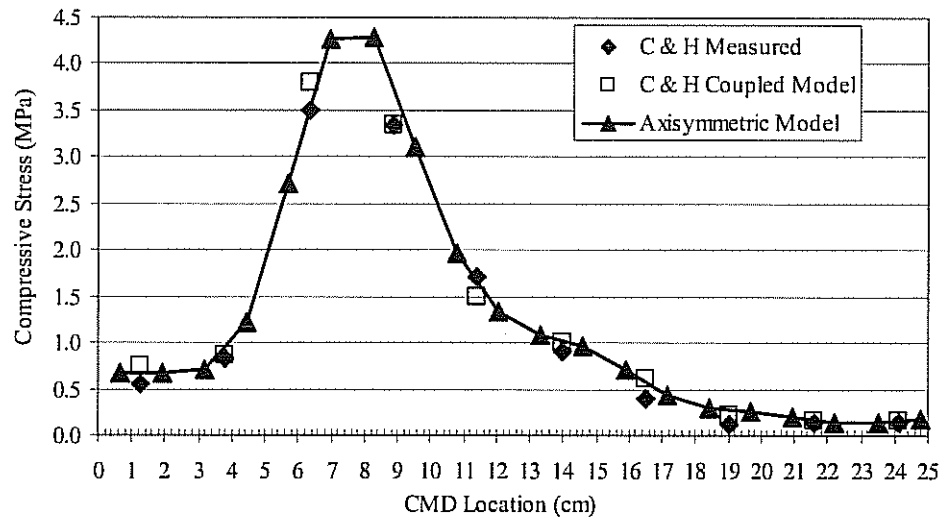

Figure 6 - Cole and Hakiel [8] Measured and Modeled Core Pressure verses Axisymmetric, Tension Allocation Model.

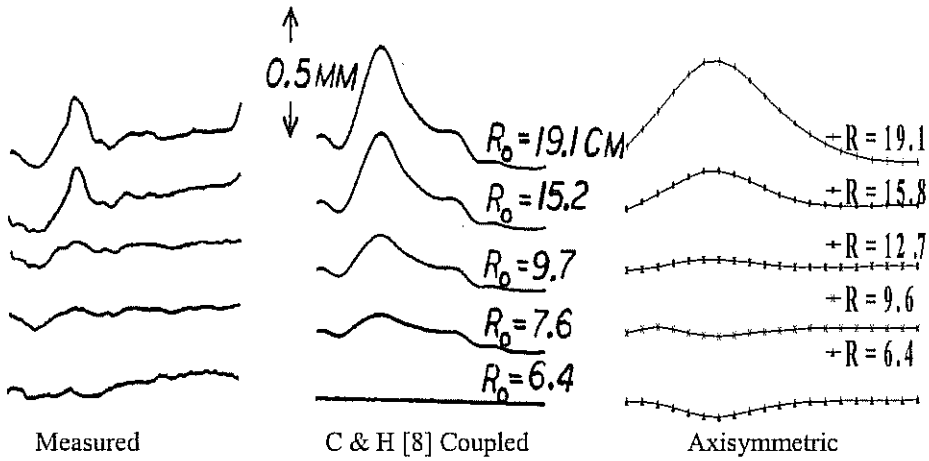

Figure 7 – Radial Profile Comparison Between Cole and Hakiel [8] Measured and Modeled Values Against the Axisymmetric, Tension Allocation Model.

Included in the plot are Cole and Hakiel's measured values, and the values predicted by their model. The axisymmetric model comes quite close to matching the magnitude displayed in the measured radial profile. Neither model captures all the nuances of their measured profile though.

The model's outer layer circumferential stresses all during the wind reflect the radius based tension allocation. As a direct consequence of equation {10}, the stresses allocated to the outer layer are directly proportional to the roll's radius, instead of equaling the uniform web line tension. This is clearly seen in the comparison between the circumferential tension in the outer layer, and the web line tension, shown as Figure 8.

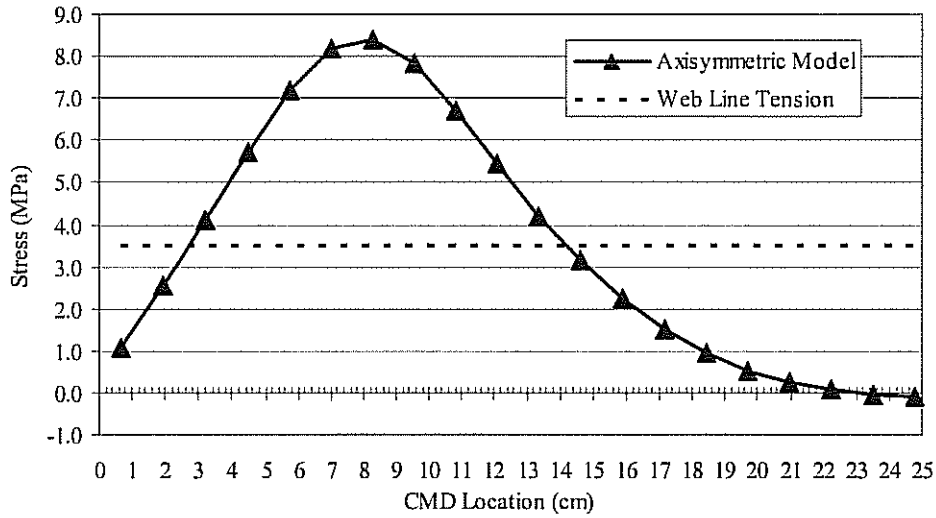

Figure 8 – Circumferential Stress Comparison Between the Input Web Line Tension and the Axisymmetric, Tension Allocation Model.

The impact and the necessity of radially allocating out the web line tension, can be seen throughout the roll, when the results are compared to those obtained using uniformly distributed tension. On the left side of Figure 9 below are the in-roll compressive radial stresses, the in-roll circumferential stresses, and the net difference in radius across the width for the radius based allocation. On the right is the same roll, but with uniform tension.

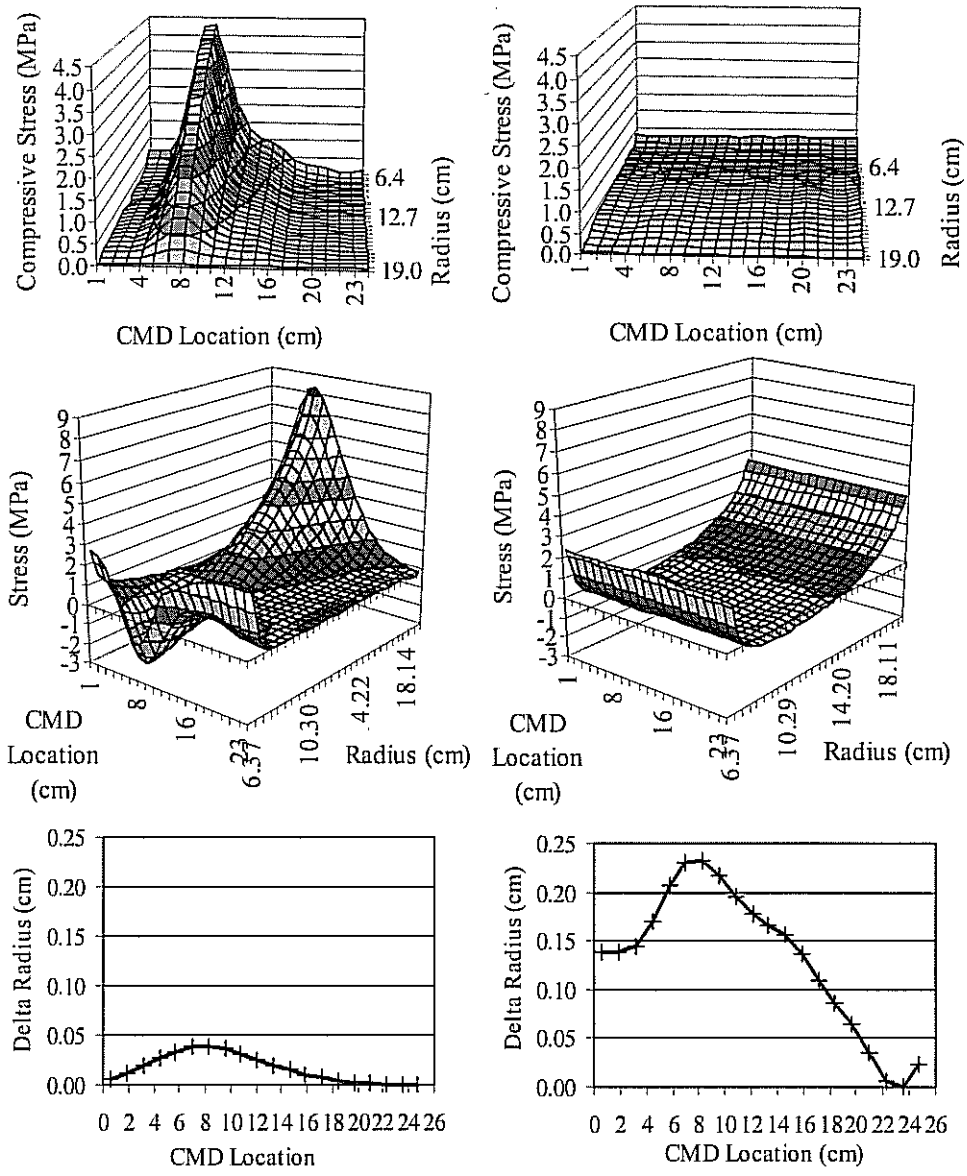

Figure 9 – Radius Based Tension Allocation verses Uniform Tension Allocation.

The plots could hardly be any more different. The compressive stress at the core is six times greater for the radius based results. And, for the circumferential stresses, the radius based allocation produces a large compressive region at the core. Finally, the delta radius plots show that the tension concentration in the thicker CMD location produces enough compression that the outside of the roll ends up fairly uniform. Thus a visual inspection could lead to a false conclusion of uniformity.

CONCLUSIONS

Overall, the three dimensional, axisymmetric, finite element model displays promising results. It utilizes the non-linear radial modulus, and captures the stress behavior seen in experiments and other models. It produces a realistic radial profile across a non-uniform wound roll. It is versatile enough to be used for numerous webs and configurations, that it represents a practical tool for the industry. The formulation is also expandable making it an attractive foundation for further research. Indeed, the model readily provides the stresses and radii throughout a wound roll, thereby giving a complete picture of it. As witnessed via the segments being narrower than for Cole and Hakiel's instrumented core, the model offers precision too.

Most importantly, the model's close agreement to experimental results shows that it is properly handling the allocation of the web line tension. The tension cannot allocate uniformly at each CMD thickness location, and still produce the compressive radial stress values seen. Instead, the thickness variations across the width concentrate the stress wound into the roll, into those locations which have the largest radii.

REFERENCES

1. Pfeiffer, J. David, "Internal Pressures in a Wound Roll of Paper.", TAPPI Journal, Vol. 49, No. 8, August 1966, pp. 342-347.
2. Altmann, Heinz C., "Formulas for Computing the Stresses in Center-Wound Rolls.", TAPPI Journal, Vol. 51, No. 4, April 1968, pp. 176-179.
3. Gutterman, R. P., "Theoretical and Practical Studies of Magnetic Tape Winding Tensions and of Environmental Roll Stability," Contract # DA18-119-SC-42, General Kinetics, Inc., Arlington, Virginia, 1959.
4. Hakiel, Z., "Nonlinear Model for Wound Roll Stresses," TAPPI Journal, Vol. 70, No. 5, May 1987, pp. 113-117.
5. Good, J. K., and Pfeiffer, J. D., "Tension Losses during Centerwinding," Proceedings of the 1992 TAPPI Finishing and Converting Conference, pp. 297-306.
6. Kedl, D. M., "Using A Two Dimensional Winding Model to Predict Wound Roll Stresses that Occur Due to Circumferential Steps in Core Diameter or to Cross-Web Caliper Variation," Proceedings of the First International Conference on Web Handling, Oklahoma State University, 1991.
7. Hakiel, Z., "On the Effect of Width Direction Thickness Variations in Wound Rolls," Proceedings of the First International Conference on Web Handling, Oklahoma State University, 1991.
8. Cole, K., and Hakiel, Z., "A Nonlinear Wound Roll Stress Model Accounting for Widthwise Web Thickness Nonuniformities," ASME, Applied Mechanics Division, Vol. 149, ASME 1992.
9. Lee, Y.M., and Wickert, J.A., "Stress Field in Finite Width Axisymmetric Wound Rolls," Submitted for Publication in Transactions of the ASME, Journal of Applied Mechanics, 2002.

10. Lee, Y.M., and Wickert, J.A., "Width-Wise Variation of Magnetic Tape Pack Stresses," Transactions of the ASME, Journal of Applied Mechanics, Proof Copy, Vol.69, May 2002, pp.1-12.
11. Chandrupatla, T. R., Belegundu, A. D., Introduction to Finite Elements in Engineering, 2nd Edition, Prentice-Hall, Inc., 1997.
12. Lekhnitskii, S. G., Anisotropic Plates, Gordon and Breach, Science Publishers, Inc., 1968, pp. 106-110.

Name & Affiliation	**Question**
Herong Lei Eastman Kodak	First, Paul, it is a very nice job. My question is that in the paper if you look at the thickness variation, it is not very much across the web. But in real manufacturing, when we wind our rolls, we put knurls on the edges. The thickness of the knurls is significantly higher than the PET web. In that winding process, we generate a lot of gapping in the middle area of the roll. I did not hear you talk about that in your model. Can your model handle that gapping? If you do, how did the finite element handle that kind of a problem, because the finite element is based on the continuous media, but now we have gapping there.
Name & Affiliation	**Answer**
Paul Hoffecker Oklahoma State University	Yes, the next generation of this model does include gapping considerations. It causes all kinds of instability; it causes much more iteration requirements on getting everything to converge properly. It is in there, but it would take a long time to discuss. Maybe offline would be a better time to discuss this with you. But, yes, we did have that as part of our considerations.
Name & Affiliation	**Answer**
Keith Good Oklahoma State University	In Paul's model each layer of web that is wound on has it own separate nodes. You are right, generally in finite elements, we are modeling a continuum. But if when he enforces the Lagrangian constraints, if there is in fact a gap there, the two nodes that would join from one layer to the next layer are not forced to coexist. The gap can exist.
Name & Affiliation	**Question**
Herong Lei Eastman Kodak	So you have zero pressure then, basically.
Name & Affiliation	**Answer**
Keith Good Oklahoma State University	Correct.